Terahertz quantum-cascade lasers with resonant-phonon depopulation: high-temperature and low-frequency operation

S. Kumar*, B. S. Williams†, Q. Qin*, A. W. M. Lee*, Q. Hu*, J. L. Reno‡, Z. R. Wasilewski§ and H. C. Liu§
*Massachusetts Institute of Technology
Department of Electrical Engineering and Computer Science and Research Laboratory of Electronics
Cambridge, MA 02139, USA
†University of California at Los Angeles
Department of Electrical Engineering, 68-117 Engineering IV Building, 420 Westwood Plaza, Los Angeles, CA 90095, USA
‡Sandia National Laboratories
Center of Integrated Nanotechnologies, MS1303, Albuquerque, NM 87185, USA
§Institute of Microstructural Sciences
National Research Council, Ottawa, Ontario, K1A 0R6, Canada

***Abstract*—Our latest results on the development of terahertz quantum-cascade lasers for high-temperature and low-frequency operation are reported. The designs are based on a resonant-phonon depopulation scheme and metal-metal waveguides are used for mode confinement. Pulsed operation up to a heat-sink temperature of** 169 K **at** $\nu \sim 2.7$ THz **and** 165 K **at** $\nu \sim 4.1$ THz **is demonstrated with a two-well injector design. For operation at lower frequencies, a one-well injector based design is developed, which reduces optical losses due to intersubband absorption in the injector region. A laser operating at** $\nu = 1.59$ THz **(**$\lambda = 188.5$ μm**) up to a heat-sink temperature of** 71 K **in continuous-wave mode is demonstrated for such a design.**

I. Introduction

Terahertz (THz) quantum-cascade lasers (QCLs) [1] have rapidly covered the frequency range of $1.6 - 5.0$ THz ($\lambda \sim 190 - 60$ μm). They have already been demonstrated in applications such as imaging, spectroscopy, and as local oscillators in heterodyne receivers. There is a strong effort currently to increase their operating temperatures so that cryogenic operation may not be needed. Also, efforts are underway to obtain robust operation at $\nu < 2$ THz, partly due to the allure of this region of spectrum for THz imaging over long distances, and also because no efficient coherent solid-state source exist that operate near and above 1 THz.

II. High temperature operation

The designs for temperature performance are based on modifications of the original design with the resonant-phonon based depopulation scheme [2], a typical conduction band diagram of which is shown in Fig. 1. Pulsed measurement results from lasers corresponding to variations of the design operating at $\nu \sim 2.7$ THz ($T_{\max,\mathrm{pul}} = 169$ K) and $\nu \sim 4.1$ THz ($T_{\max,\mathrm{pul}} = 165$ K) are shown in Figs. 2 and 3, respectively. Record high $T_{\max}$ values are obtained for both the devices, attesting to the versatility of this design in terms of spectral coverage without compromising the temperature performance.

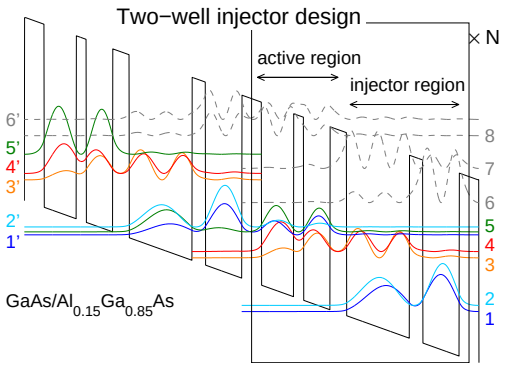

Fig. 1. Two-module conduction band diagram for the two-well injector design. The radiative transition is from $5 \rightarrow 4$ ($h\nu \approx E_{54}$) and $E_{32} \approx \hbar\omega_{\mathrm{LO}}$.

The primary temperature degradation mechanisms in this design are perceived to be the reduction in the lifetime of the upper radiative level 5 due to LO-phonon mediated $5 \rightarrow 4$ scattering, and also due to the $5' \rightarrow 8$ coupling, both of which are thermally activated processes. This is affirmed by the fact that the FL183R-2 laser (Fig. 3) with design values of $E_{54} \sim 19$ meV and $E_{5'8} \sim 8$ meV has a stronger J_{th}-T variation as compared to the FL178C-M10 laser (Fig. 2) with the corresponding design values of $E_{54} \sim 13$ meV and $E_{5'8} \sim 14$ meV. The present temperature performance in these designs has been obtained by maximizing $J_{\max}/J_{\mathrm{th}}$, affected by reduction in the the low-bias parasitic current channels and by improvement in the injector transport [3].

III. Low-frequency operation

To extend the operation of the resonant-phonon designs to lower frequencies, a one-well injector based design has been developed [5]. The active region in a QCL has higher losses at lower frequencies due to intersubband optical absorption

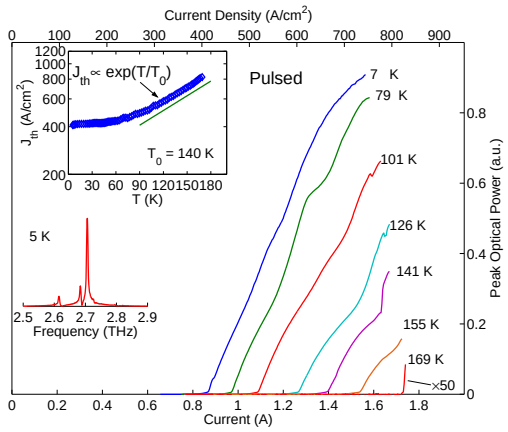

Fig. 2. Pulsed measurement results from a 100 μm × 2.1 mm metal-metal (Cu-Cu) waveguide ridge laser with cleaved facets. The design, named as FL178C-M10, is nominally similar to the one in Ref. [3]. The spectrum in the inset is from a different but similar device since the original device was accidentally destroyed during the measurements.

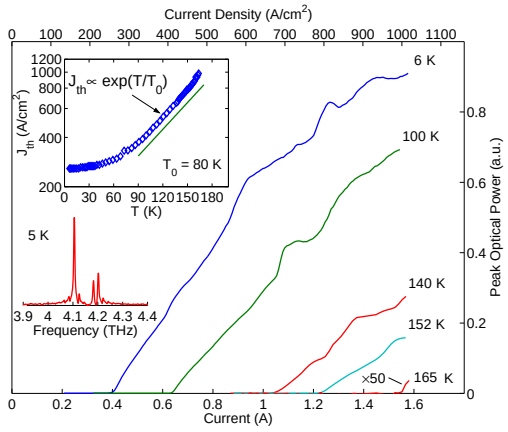

Fig. 3. Pulsed measurement results from a 80 μm × 1.94 mm metal-metal (Cu-Cu) waveguide ridge laser with cleaved facets. The active region design and the MBE wafer, named as FL183R-2, is the same as in Ref. [4].

in the injector region. A one-well injector scheme minimizes these losses due to the absence of any additional levels in the injector where majority of the electrons are localized.

The conduction band diagram and experimental results for a design operating at $\nu \sim 1.6$ THz are shown in Figs. 4 and 5, respectively. The primary challenge in this design is to minimize the low-bias parasitic current channels (predominantly due to $1' \rightarrow 2$ coupling), which can cause premature occurrence of a negative-differential resistance (NDR) region, thereby preventing the device from reaching the design bias [5]. The low-bias current channels become even stronger in a lower frequency design. As a consequence, the lasing range $J_{\max}/J_{\rm th}$ for the device in Fig. 5 is very small. Nevertheless, this device lased up to a value of $T_{\max,\rm cw} \sim 71$ K and more than 0.65 mW of optical power was detected with a thermopile detector in continuous-wave (cw) operation. A more robust operation at even lower frequencies can be expected in a future design iteration because this design

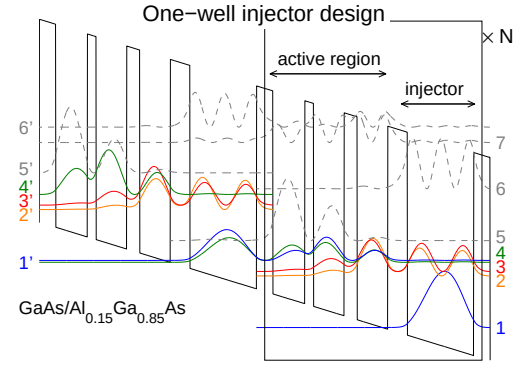

Fig. 4. Two-module conduction band diagram for the one-well injector design. The radiative transition is from $4 \rightarrow 3$ ($h\nu \approx E_{43}$) and $E_{21} \approx \hbar\omega_{\rm LO}$.

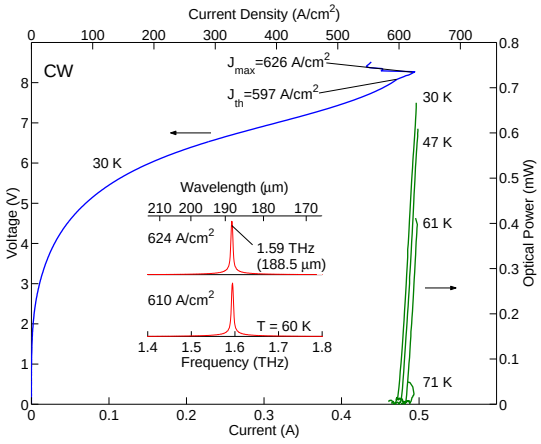

Fig. 5. CW measurement results from a 76 μm × 1.04 mm metal-metal (Cu-Cu) waveguide ridge laser with cleaved facets. The design, named as OWI180B, is a modified version of the one in Ref. [5].

was grown in a different MBE machine as compared to the one in Ref. [5], whereby some design readjustments may be needed due to a possible variation in the Al content of the $\rm Al_{0.15}Ga_{0.85}As$ barriers from one machine to another.

ACKNOWLEDGMENT

This work is supported by AFOSR, NASA, and NSF. Sandia is a multiprogram laboratory operated by Sandia Corporation, a Lockheed Martin Company, for the U.S. Department of Energy under Contract DE-AC04-94AL85000.

REFERENCES

[1] R. Köhler, A. Tredicucci, F. Beltram, H. E. Beere, E. H. Linfield, A. G. Davies, D. A. Ritchie, R. C. Iotti, and F. Rossi, "Terahertz semiconductor-heterostructure laser," *Nature*, vol. 417, p. 156, 2002.

[2] B. S. Williams, H. Callebaut, S. Kumar, Q. Hu, and J. L. Reno, "3.4-THz quantum cascade laser based on longitudinal-optical-phonon scattering for depopulation," *Appl. Phys. Lett.*, vol. 82, p. 1015, 2003.

[3] B. S. Williams, S. Kumar, Q. Hu, and J. L. Reno, "Operation of terahertz quantum-cascade lasers at 164 K in pulsed mode and at 117 K in continuous-wave mode," *Opt. Express*, vol. 13, p. 3331, 2005.

[4] ——, "High-power terahertz quantum-cascade lasers," *Electron. Lett.*, vol. 42, p. 89, 2006.

[5] S. Kumar, B. S. Williams, , Q. Hu, and J. L. Reno, "1.9 THz quantum-cascade lasers with one-well injector," *Appl. Phys. Lett.*, vol. 88, p. 121123, 2006.